Piezoelectric-Driven Self-Charging Supercapacitor Power Cell

Ananthakumar Ramadoss,[†,¶] Balasubramaniam Saravanakumar,[‡,¶] Seung Woo Lee,[§] Young-Soo Kim,[∥] Sang Jae Kim,[*,†,‡,∥] and Zhong Lin Wang[∥,⊥]

Nanomaterials and System Lab, [†]Faculty of Applied Energy System, Science and Engineering College, and [‡]Department of Mechatronics Engineering, Engineering College, Jeju National University, Jeju City, Jeju 690-756, Republic of Korea, [§]Woodruff School of Mechanical Engineering and [∥]School of Materials Science and Engineering, Georgia Institute of Technology, Atlanta, Georgia 30332-0245, United States, and [⊥]Beijing Institute of Nanoenergy and Nanosystems, Chinese Academy of Sciences, Beijing, China. [¶]These authors contributed equally.

ABSTRACT In this work, we have fabricated a piezoelectric-driven self-charging supercapacitor power cell (SCSPC) using MnO_2 nanowires as positive and negative electrodes and a polyvinylidene difluoride (PVDF)—ZnO film as a separator (as well as a piezoelectric), which directly converts mechanical energy into electrochemical energy. Such a SCSPC consists of a nanogenerator, a supercapacitor, and a power-management system, which can be directly used as a power source. The self-charging capability of SCSPC was demonstrated by mechanical deformation under human palm impact. The SCSPC can be charged to 110 mV (aluminum foil) in 300 s under palm impact. In addition, the green light-emitting diode glowed using serially connected SCSPC as the power source. This finding opens up the possibility of making self-powered flexible hybrid electronic devices.

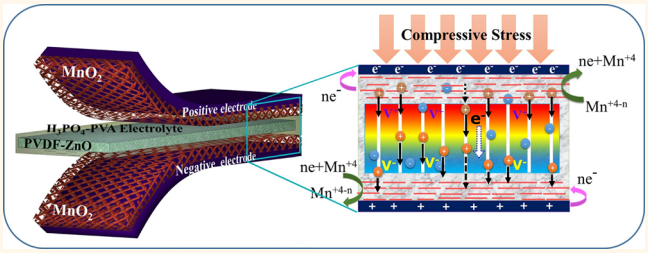

KEYWORDS: self-charging · energy storage · energy harvesting · piezoelectric separator

A rapidly developing worldwide economy has triggered serious global warming and the lack of fossil fuels, which possess significant threats to the survival and development of mankind.[1−4] To address these issues, scientists and engineers have been conducting intense research efforts into the design and fabrication of efficient energy conversion and storage devices to exploit sustainable and clean energy.[1] Usually, energy harvesting and storage are two different processes that are performed through two different techniques and separated physical units.[5−8]

Among the conversion methods, a nanogenerator is an effective device tool to harvest low-frequency mechanical energy through piezoelectric and tribo-electrification processes.[9−15] On the other hand, electrochemical capacitors (ECs) or supercapacitors are considered to be one of the most important next-generation energy storage devices, mainly due to their high power density, fast charge−discharge rates, and long life times compared to rechargeable batteries and conventional dielectric capacitors.[16−19] Such a device can be used as a primary power storage source or auxiliary power storage source with rechargeable batteries in electric vehicles and other electronic devices for the purpose of power enhancement. Different types of energy conversion and storage devices are available in the market. Researchers are trying to develop a new hybrid system by integrating an energy harvesting device along with a storage device to perform a self-powered operation. Recently, a new concept of a self-charging power cell was introduced,[20−25] in which the mechanical energy is directly converted into electrochemical energy *via* a piezoelectric effect and is directly stored in a Li-ion battery. In addition, Pankratov *et al.*, reported a new kind of electric power hybrid device (self-charging electrochemical biocapacitor), in which chemical energy could be directly converted into electrochemical energy.[26−28]

Rapid growth of portable electronic devices such as mobile phones, tablets, bendable displays, portable electronic papers, wearable personal multimedia, and some medical devices has prompted researchers to look for thin, lightweight, and flexible energy storage technologies. Therefore, flexible

* Address correspondence to kimsangj@jejunu.ac.kr.

Received for review February 3, 2015 and accepted March 20, 2015.

Published online 10.1021/acsnano.5b00759

all-solid-state supercapacitors have been established by sandwiching the gel electrolyte between positive and negative electrodes on flexible substrates. When compared to the conventional supercapacitors having liquid electrolytes, the solid-state supercapacitors made of gel-type electrolyte play a dual role of electrolyte and separator. Moreover, unlike the conventional supercapacitors, the solid-state capacitors avoid the possibility of electrolyte leakage and also the short circuit of two electrodes. In this context, a simplified and low-cost method to fabricate a flexible self-charging supercapacitor power cell is greatly desired for portable applications.

Herein, we first attempted to fabricate a piezoelectric-driven self-charging supercapacitor power cell (SCSPC) device using polyvinylidene difluoride (PVDF)—ZnO as a piezoelectric as well as a separator, poly(vinyl alcohol)—phosphoric acid (PVA—H_3PO_4) as a gel electrolyte, and electrochemically active manganese oxide (MnO_2) nanowires as positive and negative electrodes. Among the various metal oxides, MnO_2 exhibits intriguing properties such as high theoretical specific capacitance (~1400 F g^{-1}), low cost, and environmental friendliness, suggesting it may be a promising electrode material for supercapacitors.[29−33] The fabrication and working mechanism of a SCSPC is discussed in detail.

RESULTS AND DISCUSSION

The fabricated SCSPC is schematically represented in Figure 1a. The device consists of three components: a positive electrode, a separator, and a negative electrode. The MnO_2 nanowires/conductive carbon/binder mixtures on aluminum foil were used as the positive and negative electrodes. The PVDF—ZnO film was used as a separator (as well as a piezoelectric) instead of a conventional separator. Further, Figure 1b shows the optical images of fabricated SCSPC (aluminum foil and fabric).

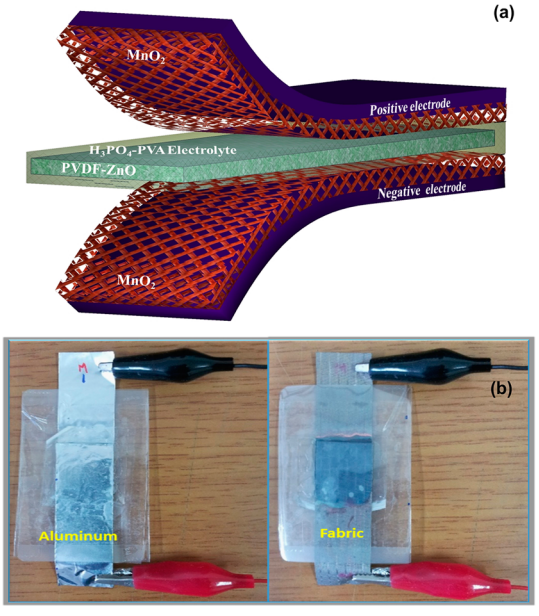

Figure 1. (a) Schematic diagram of the fabricated SCSPC. MnO_2 on aluminum foil is used as the positive and negative electrodes and PVDF—ZnO film as a separator. (b) Digital images of SCSPC based on aluminum foil and conductive fabric.

Mechanism of Self-Charging Supercapacitor Power Cell. The working mechanism of the SCSPC is based on piezoelectric potential-driven electrochemical oxidation and reduction reaction (faradaic reaction).[20−22] The fabricated SCSPC (Figure 2) consists of piezoelectric material (PVDF—ZnO film) as a separator as well as a potential generator, MnO_2 nanowires as positive and negative electrodes for the electrochemical reaction, and PVA/H_3PO_4 as the electrolyte, which is uniformly distributed through the entire surface of the separator and the surface of the electroactive materials. At the beginning, the device is at the discharge state (Figure 2a), in which there is no electrochemical reaction due to the electrochemical equilibrium between the electrolyte and electrodes (active material). At this stage, there is no external deformation applied to the device. A compressive stress was applied to the device by means of palm impact from the top side of the device (Figure 2b), which caused the polarization of the PVDF film by the piezoelectric effect.[20−22] The polarization of ions generates a potential difference across the thickness of the separator (PVDF—ZnO). A positive and negative piezoelectric potential was generated at the top and the bottom side of the film, driving the electrolytic ions (PVA/H_3PO_4) toward the positive and negative electrodes. The piezoelectric field induced cationic (H^+) movement in the electrolyte to screen the generated piezopotential across the separator (ionic conduction path is represented in Figure 2b). This ionic movement induces an electrochemical imbalance in the electrolyte and the positive and negative electrode sides. To obtain chemical equilibrium, the oxidation and reduction reactions (faradaic) occur at the surfaces of the positive and negative electrodes (Figure 2c), respectively.

The migration of H^+ ions from the electrolyte toward the negative electrode leads to the reduction reaction in $(MnO_2)_{surface}$ through H^+ ion insertion (without disruption of the oxide lattice) and builds the positive charges at the negative electrode (Al foil). Meanwhile, the oxidation reaction occurs at the positive electrode through the H^+ ion desertion, which leaves free electrons to the current collector at the positive electrode side (Al foil). The electrochemical reaction can be expressed as follows:[30]

$$MnO_2 + H^+ + e^- \leftrightarrow MnOOH \quad (1)$$

The liberated electrons are transported to the negative electrode to maintain the charge neutrality as well as the continuity of the charging process.

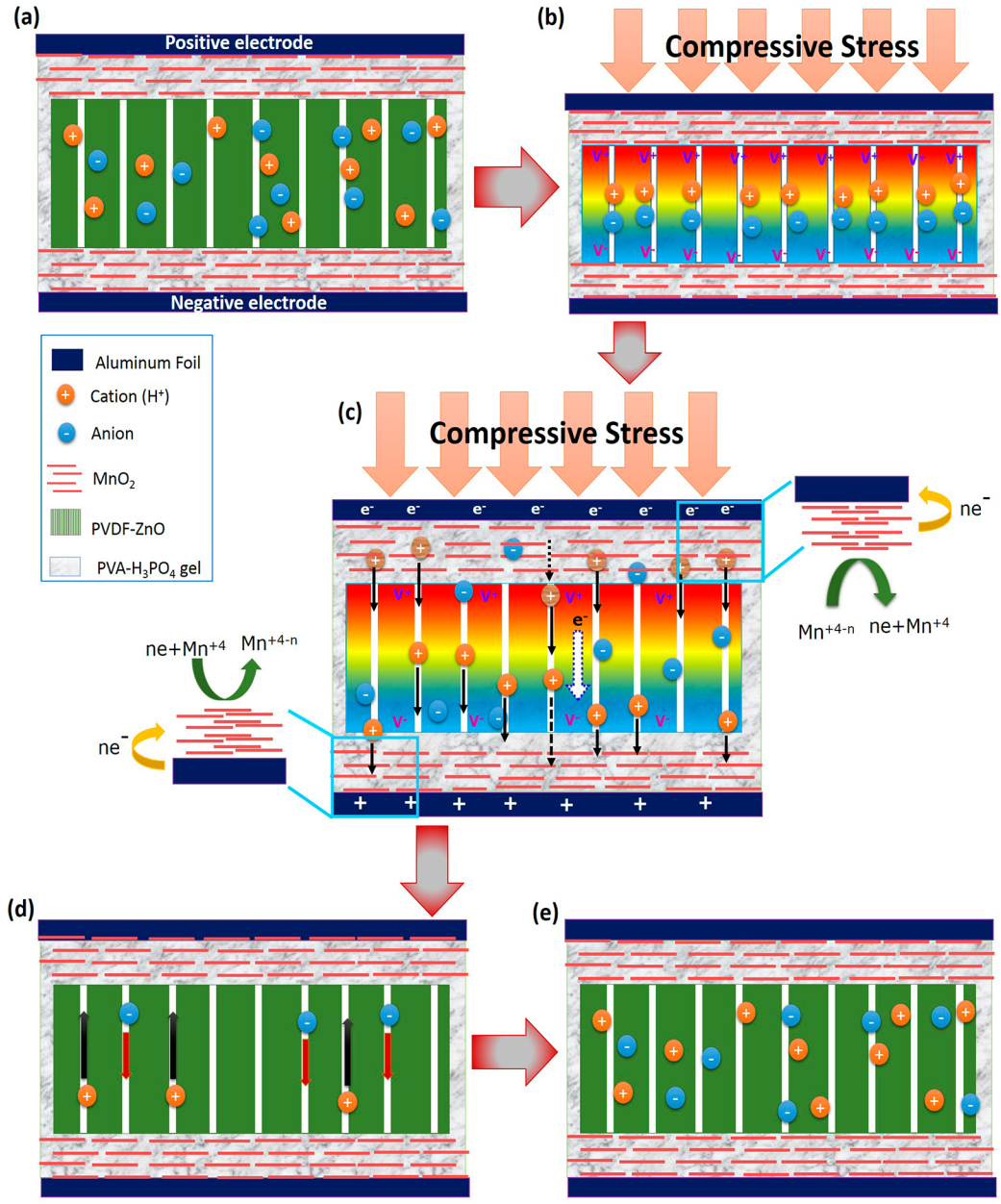

Figure 2. Working mechanism of the SCSPC driven by mechanical deformation. (a) Fabricated SCSPC at the discharge condition. (b) Mechanical deformation is applied on the top of the device; it creates a piezoelectric field (potential) in the PVDF−ZnO separator film. (c) Under the piezoelectric field, the H^+ ions will migrate through the PVDF−ZnO separator in the electrolyte to the negative electrode, leading to the corresponding charging reactions at the two electrodes. (d) When external deformation is released, there is no piezoelectric field at the separator, which breaks the attained chemical equilibrium; it causes a reverse reaction on both sides of the electrode, and ions are relocated into the original position. (e) Completed self-charging cycle.

There are two possibilities for the electron transfer; one is inside the SCSPC, and another is through the external circuit *via* a monitoring system (electrochemical workstation).[20−22] In order to verify the electron flow in the SCSPC, we have directly measured the stored voltage through a multimeter before and after compression without any external circuit/monitoring system. The open-circuit voltage was found to increase under repeated compression, clearly indicating the self-charging process of SCSPC. From this study, we concluded that the electron may flow through the inside of the device. The detailed mechanisms of electron flow inside the SCSPC are still under debate. In such a SCSPC, the charging process involves cation insertion into the negative electrode surface and desertion from the positive electrode surface.

Under continuous compression force, the charging process was repeated to attain chemical equilibrium of the two electrodes with piezoelectric potential; at this point, there is no further ionic polarization in the device. This is the process of converting mechanical energy directly into electrochemical energy.

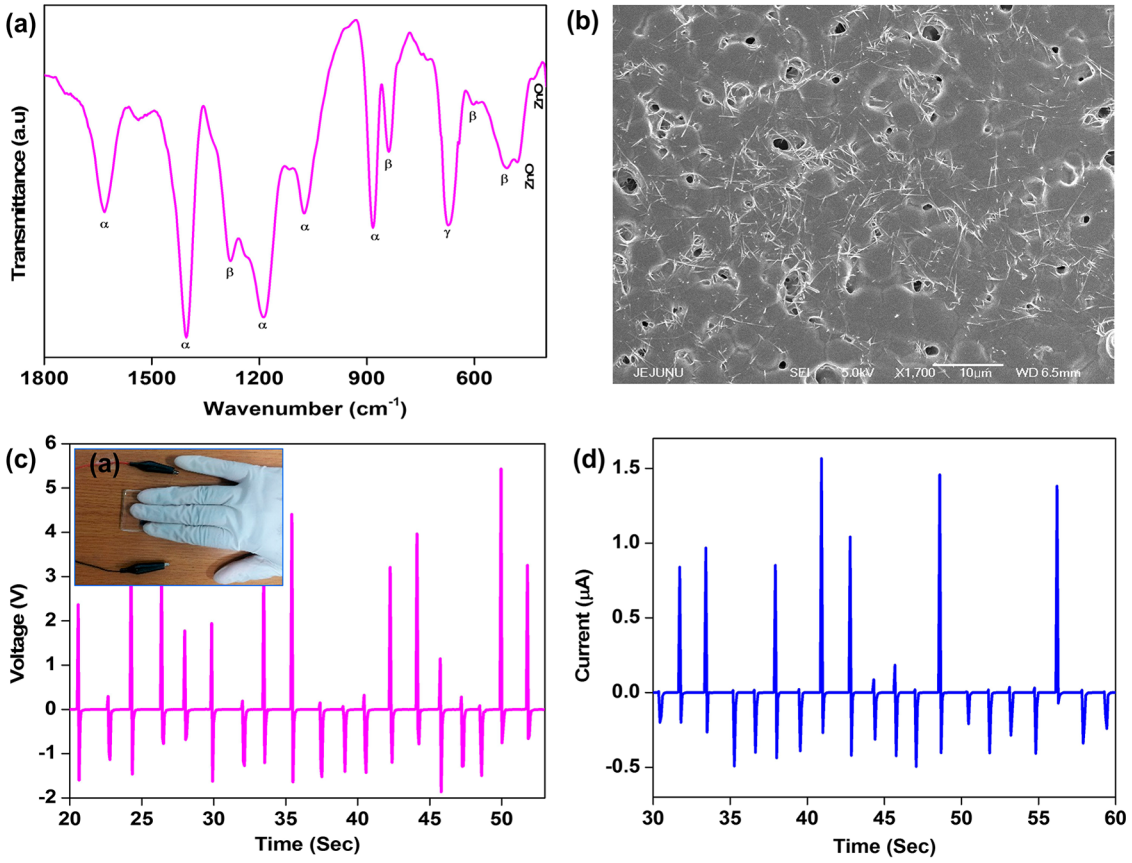

Figure 3. (a) FT-IR spectrum and (b) FE-SEM image of the PVDF−ZnO separator. The β-phases of PVDF and ZnO stretching vibrations are indexed. Open-circuit voltage (c) and short-circuit current (d) generated in the PVDF−ZnO separator. The inset shows the digital image of a fabricated PVDF−ZnO nanogenerator device. The average output voltage and current is 5 V and 2 μA, respectively. The output voltage and current of the device were not uniform, which may be attributed to different strain rates.

When removing the compression force, piezoelectric potential disappeared in the PVDF film (Figure 2d); it breaks the electrochemical equilibrium of the device. To compensate, a small amount of ions will move back, indicating the completion of the charging cycle. When a charging cycle is completed through the electrochemical reaction (Figure 2e), a small oxidation and reduction occurred at the positive and negative electrode surfaces. With continuing applied force to the device, the charging cycle is repeated, which results in a conversion of mechanical energy directly into electrochemical energy. From the above discussion, it could be argued that there are three main processes occurring in the self-charging process: the generation of piezoelectric potential on a PVDF−ZnO film by palm impact, the migration of ions toward electrodes through an ionic conduction path, and the reduction (negative electrode) and oxidation (positive electrode) reactions occurring at MnO_2 *via* insertion/desertion of H^+ ions.

The self-charging mechanism can also be explained by using the Nernst equation, which shows the relationship between electrode potentials and H^+ concentration.[20,21,34] When the piezoelectric field is formed by external compression, H^+ ions migrate from the positive (*i.e.*, MnO_2 in the oxidation process) to the negative (*i.e.*, MnO_2 in the reduction process) electrode. As a consequence, the concentration of H^+ on the oxidative electrode decreases and the increase in H^+ concentration on the reductive electrode is simultaneously constructed. As this change of H^+ concentration electrochemically causes the potential of the negative electrode to be larger than that of the positive electrode, the device is finally self-charged by the change of redox potential through the concentration gradient of H^+ ions. The basic characteristics of the separator and electrode materials are discussed below.

Characterization of Piezoelectric Materials (Separator and Power Source). The Fourier transform infrared (FT-IR) spectrum (Figure 3a) confirmed the presence of the β-phase of PVDF at 512, 606, 838, and 1282 cm^{-2} and ZnO stretching vibration mode peaks at 518 and 420 cm^{-1}; the remaining peaks were related to other phases of PVDF.[35] Figure 3b displays the field-emission scanning electron microscopy (FE-SEM) image of the PVDF−ZnO separator, which confirms the homogeneous distribution of ZnO nanowires in crystalline superulites of the PVDF matrix. Further, the nanogenerator (energy harvesting) device was fabricated using PVDF−ZnO film with Au as top and bottom electrodes.

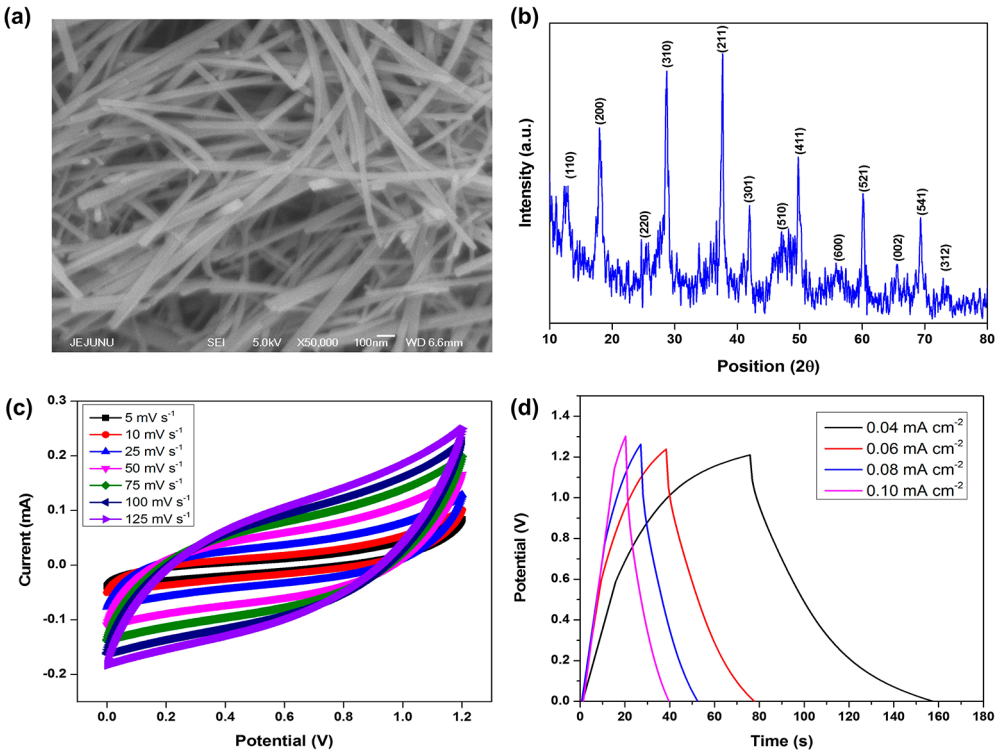

Figure 4. (a) FE-SEM image of MnO_2 nanostructure. It shows the uniform and high quality of nanowires. (b) X-ray diffraction spectrum of MnO_2 nanowires. The MnO_2 exhibited the tetragonal structure. Electrochemical performance of the SCSPC device in PVA/H_3PO_4 gel electrolytes: (c) cyclic voltammetry scans of SCSPC at different scan rates. (d) Galvanostatic charge/discharge curves of SCSPC at different current densities. The charge/discharge curves were similar in shape between 0 and 1.2 V, indicating that the device could stably perform in various current densities and further confirming the capacitive and fast charge/discharge properties of SCSPC.

Under the mechanical deformation, the piezoelectric potential was generated on the surface of PVDF−ZnO film due to the polarization of PVDF as well as ZnO. The generated output voltage is represented in Figure 3c. To compensate for the piezopotential, a transient flow of free electrons in an external circuit[36] is shown in Figure 3d. The inset of Figure 3c shows the fabricated PVDF−ZnO nanogenerator device. The presence of ZnO nanowires in the PVDF matrix induces the polarization of ions in the composite film without electrical poling.[37] From these results, we concluded that our separator can generate piezopotential in the fabricated SCSPC.

Characterization of Electrode Materials. The morphology and structure of as-synthesized MnO_2 nanowires were characterized by FE-SEM, X-ray diffraction, and Raman observations. The high-magnification FE-SEM images of MnO_2 nanowires are shown in Figure 4a. The FE-SEM image revealed that the as-synthesized MnO_2 products are composed of uniform and smooth nanowires with diameters of 40−60 nm and lengths up to several micrometers. The crystal phase and crystallinity of the as-prepared MnO_2 nanowires were analyzed by X-ray diffraction and are shown in Figure 4b. All of the diffraction peaks are consistent with the tetragonal phase of MnO_2; it was confirmed by comparing with the standard data file JCPDS no. 44-0141. No impurity peaks are observed, indicating the high purity of the as-prepared products. Moreover, the strong diffraction peaks indicate that the MnO_2 nanowires are well-crystallized. The structural features of the as-synthesized products were further investigated by Raman measurement (see section B and Figure S1 in the Supporting Information). The electrochemical behavior of the MnO_2 electrode in a three-electrode system was evaluated by cyclic voltammetry (CV), galvanostatic charge−discharge (GCD), and electrochemical impedance spectroscopy (EIS) tests (see section C and Figure S2 in the Supporting Information).

Electrochemical Behavior of the Self-Charging Supercapacitor Power Cell. The supercapacitor behavior of the as-prepared SCSPC (PVDF−ZnO film separator) was investigated by the CV and GCD measurements with an operation voltage of 1.2 V. The CV scans of the fabricated SCSPC (PVDF−ZnO film separator) at a potential window of 0 to 1.2 V are shown in Figure 4c. These CV curves exhibit rectangular-like shapes, indicating the ideal capacitive behavior. The GCD curves of the SCSPC at different current densities exhibit linear and symmetric behavior, indicating the capacitive and fast charge/discharge properties (Figure 4d). The specific capacitance of the SCSPC device was 455 mF g^{-1} at 0.04 mA cm^{-2}. The suitability of this SCSPC device for supercapacitor applications was further estimated by

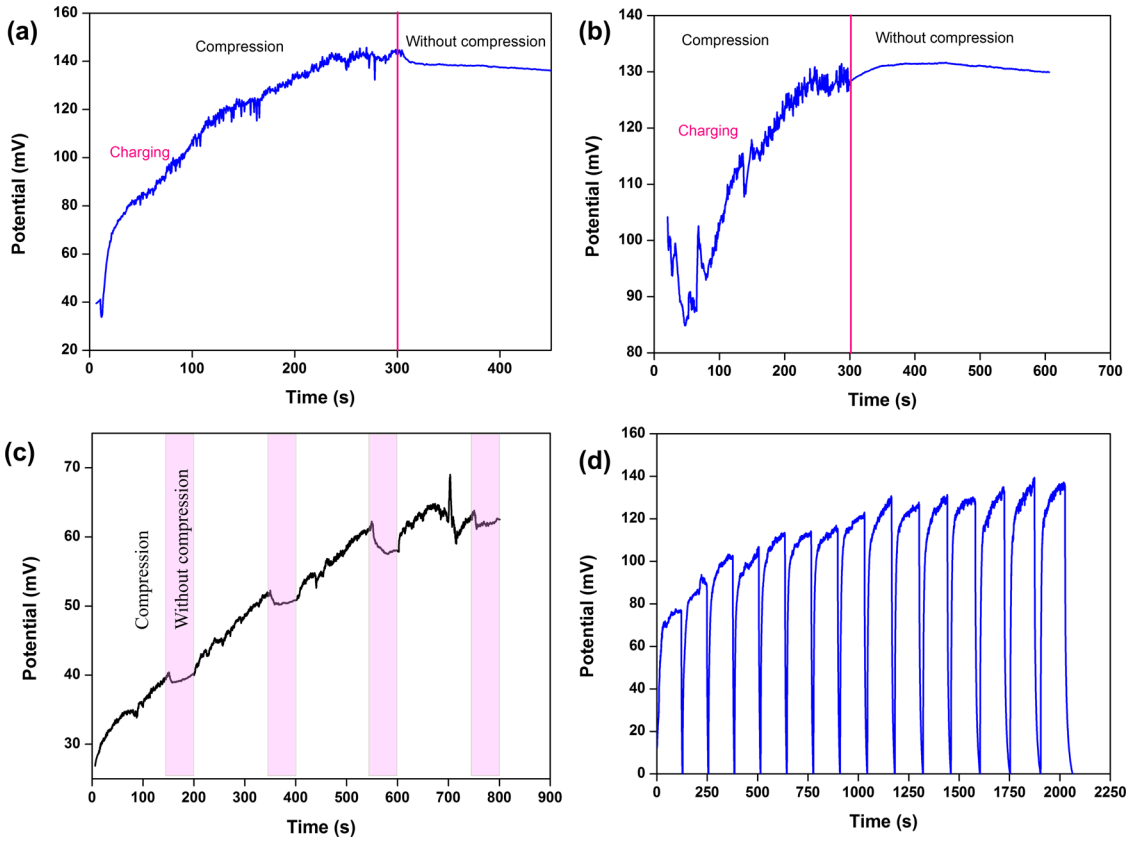

Figure 5. Self-charging performance of SCSPC monitored using an electrochemical workstation under periodic compressive straining: (a) Self-charging process of the SCSPC by human palm impact. During vibration, the voltage continues to increase, indicating that the charging process occurs due to the migration of the ions. (b) Self-charging process of the fabric-based SCSPC. (c) Cycling performance of the SCSPC under compressive force. (d) Self-charging and discharging cycles of the SCSPC *via* periodic deformation. The discharge current is 10 μA.

examining its power and energy densities. The power and energy densities were calculated using eqs 4 and 5 and the charge/discharge curves at different current densities (see section G in the Supporting Information). The energy density of the SCSPC reached 91 mW h kg^{-1} at a power density of 3.9 kW kg^{-1} and sustained 58 mW h kg^{-1} at a power density of 9.9 kW kg^{-1}. After that, the leakage current of the device was measured at a constant potential of 1.2 V for 8000 s, which is shown in Figure S3 (see section D in the Supporting Information). At the beginning, the current was suddenly dropped from 0.2 mA to 22 μA at 15 min, and then the leakage current was stabilized to ~15 μA over 8000 s. The existence of a small leakage current may be due to the presence of impurities in electrode materials or electrolyte of the fabricated SCSPC device.[38−41] For reference, we have also tested the electrochemical performance of an all-solid-state symmetric supercapacitor based on filter paper separator (see section E and Figure S4a,b in the Supporting Information). These results confirm that the proposed structure of SCSPC is fully eligible to act as a supercapacitor system.

Self-Charging Performance of As-Fabricated SCSPC. To show the self-charging capability of the SCSPC (aluminum foil), we have performed the self-charging process under continuous palm impact for 300 s, the result of which is shown in Figure 5a. When a compressive force is applied to SCSPC, the voltage of the device increases from 35 to 145 mV (110 mV charged) in 300 s. After the compression force was removed, the stored energy was sustained for approximately 150 s, and then again when deformation was applied to the device, the voltage started to increase (see Figure 5a). This concludes that our SCSPC has the ability to self-charge under mechanical deformation/vibration. The device showed slight decrease in voltage at the initial ~25 s and then started to increase in voltage under continuous force. This may be attributed to the random movement of ions in the electrolyte solution under an external force. At the initial stage, the device becomes a non-equilibrium state (voltage decreases; discharging) due to the sudden force applied to the device. After continuous palm impact, the device attained a chemical equilibrium at the both electrode sides (faradaic reaction occurred at the electrode material surface) and started to increase the device voltage (charging) after ~25 s.

To demonstrate the flexible, lightweight, and wearable-based self-powered device applications,

we have fabricated and tested the self-charging process of the fabric-based SCSPC under continuous palm impact for 300 s. Figure 5b represents the self-charging process of the fabric-based SCSPC using PVDF−ZnO separator films. Under continuous vibration, fabric-based SCSPC showed an increase in voltage (charging) from 85 to 130 mV (45 mV charged) in 300 s. After the deformation was removed, the device showed an increase in voltage for 50 s and then sustained the stored voltage for 250 s, which confirm the self-charging capability of the as-fabricated fabric-based SCSPC. The increase in voltage was observed after deformation, which may be due to the vibration that continued for a few seconds after deformation and the light weight of the fabricated fabric-based SCSPC. Both devices showed increased voltage (charging) under the continuous force, confirming the self-charging performance of the SCSPC.

The self-charging performance of the device mainly depends on applied compressive force. To verify that, we have studied the self-charging performance of SCSPC under various compressive force conditions. Varied compressive force of approximately 9.8, 12.2, 14.9, and 18.8 N was applied through a human hand (using a metal cylinder). Figure S5 shows the self-charging and discharging cycles under different compressive stress (see section F in the Supporting Information). When the applied force to SCSPC increased, the self-charging result is enhanced. The enhancement in the self-charging process is due to the increase in piezopotential with the higher applied strain (compressive force). After the self-charging process, the device was discharged back to its original voltage under a constant discharge current of 1 μA. These results confirmed that the self-charging process is due to the piezoelectric effect.

The cycling performance of the fabricated SCSPC was performed under a compressive force. As shown in Figure 5c, the voltage of the device increased (self-charging) under the compressive force (∼9.8 N) applied to the device for 150 s. After the self-charging process, the device sustained the charged voltage (highlighted in magenta color) for 50 s. Approximately, the SCSPC stored 15 mV in 150 s under compressive force. When the compressive force is repeated, the device starts to self-charge, confirming the repeatability (cycling performance) of the fabricated device. Further, Figure 5d shows the self-charging process and the discharging at a constant current of 10 μA for 15 cycles. The voltage of the device was increased under the compressive strain (∼18.8 N for 120 s), and then the device was back to its original voltage under a constant discharge current. The average self-charge voltage of the device was 110 mV in 120 s under compressive force. In addition, the specific capacitance of the SCSPC can be calculated using the discharge current, discharge time, and self-charged voltage (voltage window). The calculated device capacitance was 0.2575 F g^{-1} (257 mF g^{-1}). The increasing voltage trend was observed due the variation of applying compressive force (through human hand for which it was difficult to control the input force), and then after a few cycles, the device attained a stabilized state. This result confirms the better cycling performance (repeatability) of the fabricated SCSPC. Besides, we have checked the self-charging process of SCSPC connected to the opposite sign (polarity change), which is displayed in Figure S6 (see section F in the Supporting Information). Under vibration, the voltage of the device increased from 105 to 140 mV at a negative direction in 300 s. After deformation, the device sustained the stored energy for 100 s. This also confirms the self-charging performance of the SCSPC.

Furthermore, the self-charging capability of the five SCSPCs that are connected serially was tested under the continuous human palm impact to all devices, as shown in Figure 6a. Under continuous impact, the open-circuit voltage increases from 160 to 280 mV (120 mV charged) in 350 s and is then sustained as stored voltage for 250 s, even after removing the deformation. The inset of Figure 6a shows the photograph of serially connected SCSPCs. In addition, the compression force was applied to each one-by-one, and the self-charging capability was measured, as shown in Figure 6b. The inset in Figure 6b displays the circuit diagram for the serial connections. All of the devices show the self-charging capability when the force is applied to the individual devices. The voltage was increased from 230 to 350 mV (120 mV) in 360 s. The self-charging process mainly depended on the piezoelectric potential generation in the separator, which is directly related to mechanical deformation.

To demonstrate the potential application (self-powered devices) of these SCSPCs, we have assembled 11 SCSPCs serially to drive a light-emitting diode (LED). The required amount of potential was charged using SCSPCs as power sources. Finally, we showed that the SCSPC can drive a green LED, as displayed in Figure 6c. The inset of Figure 6c (red color border) shows the zoomed portion of the powered green LED. From the above results and discussion, we have concluded that the as-fabricated SCSPC is an initiation of new smart power electronics with self-power sources. In the future, the described method can be extended for the new nanostructured materials with high performance of redox reactions (better pseudocapacitive behavior) as well as better piezoelectric separators (highly porous film) for self-charging supercapacitor devices with further improved self-charging performances, which are currently under investigation.

CONCLUSION

In summary, we have successfully fabricated the first piezoelectric-driven self-charging supercapacitor

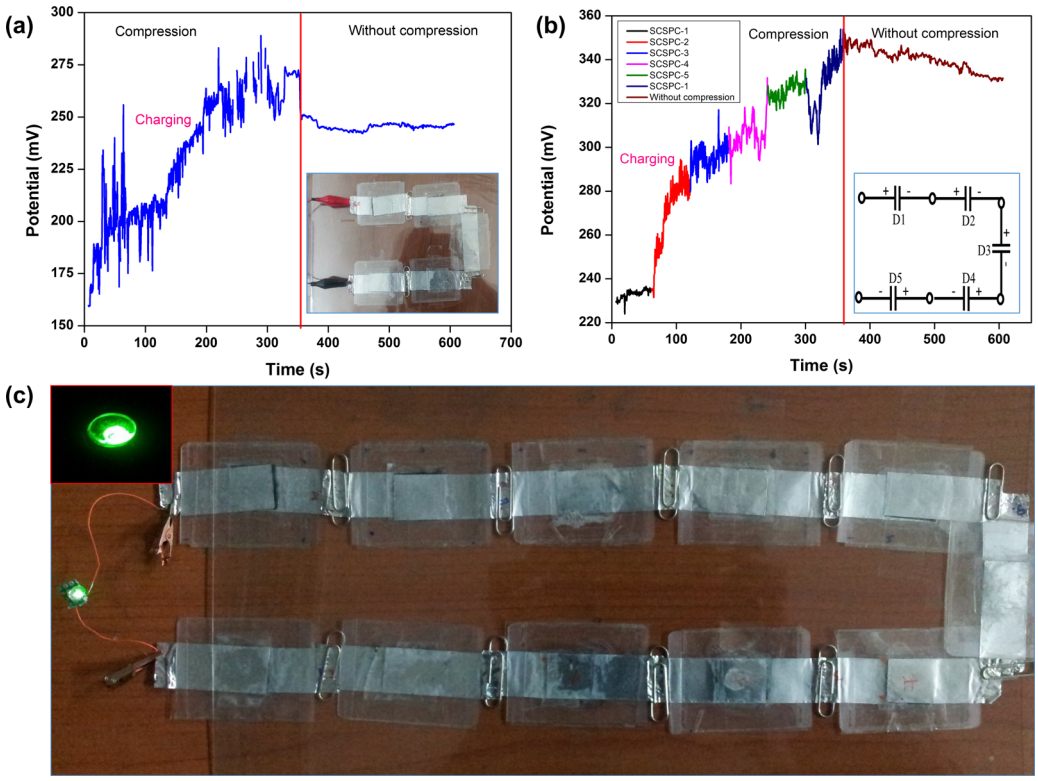

Figure 6. Self-charging performance of serially connected SCSPC: (a) self-charging process of the serially connected five SCSPCs under periodic compressive strain given by human palm impact to the whole devices. Inset shows a photograph of the serially connected SCSPCs. (b) Self-charging process of the serially connected five SCSPCs under periodic compressive straining given by human palm impact to the each device for a 60 s interval. Inset shows the circuit diagram of serial connection. (c) Operation of green light-emitting diode using serially connected SCSPCs as the power source.

power cell that consists of a PVDF–ZnO separator (piezoelectric nanogenerator) and MnO_2 nanowires used as the positive and negative electrodes (supercapacitor), which can be used to simultaneously harvest and store the mechanical energy to electrochemical energy. The SCSPC exhibited the self-charging capability under palm impact (aluminum-foil-based SCSPC = 110 mV for 300 s; fabric-based SCSPC = 45 mV for 300 s). Further, the green LED was operated using serially connected SCSPCs as the power source. The SCSPCs provide a new promising direction in supercapacitor research for the development of next-generation self-powered sustainable power sources for wearable and flexible electronic devices.

EXPERIMENTAL SECTION

Fabrication of a Self-Charging Supercapacitor Power Cell. The MnO_2 nanowires were synthesized by a hydrothermal method (see section A in the Supporting Information). The working electrodes (MnO_2) were prepared by mixing 80 wt % of active materials, 10 wt % of carbon black, and 10 wt % of PVDF in *N*-methylpyrrolidinone, and this slurry was pasted on aluminum foil as well as conductive fabric and then heat-treated at 100 °C under vacuum overnight. Then the SCSPC was assembled by two-piece MnO_2 (positive and negative) electrodes on aluminum foil with PVA/H_3PO_4 gel electrolyte separator (PVDF–ZnO) in the middle. The assembled power cell was further dried at room temperature for 12 h. Here, PVDF–ZnO acts as a separator as well as a power source (piezoelectric effect). The PVDF–ZnO film separator was prepared by a solution-casting method in a ratio of 1:0.1 (PVDF/ZnO) in dimethylformamide. The PVA/H_3PO_4 gel electrolyte was prepared by mixing 3 g of PVA in 30 mL of deionized water at 95 °C with stirring. After, the PVA was completely dissolved, and 3 g of H_3PO_4 was added into the PVA solution under vigorous stirring until it formed a homogeneous sticky solution. Then the solution was cooled at room temperature, and the solution became a clear and transparent gel. Prior to assembly, the electrodes and the separator were immersed in PVA/H_3PO_4 gel electrolyte for 5 min and then assembled one-by-one and kept at room temperature for 12 h to vaporize the excess water present in the electrolyte.

Characterization of the Self-Charging Supercapacitor Power Cell. The structure of the samples was characterized by a Rigaku X-ray diffractometer and a LabRam HR800 micro-Raman spectroscope (Horiba Jobin-Yvon, France). The morphology of the samples was investigated using FE-SEM (JSM-6700F, JEOL Ltd., 2 kV). The electrochemical and self-charging performances of the as-prepared electrodes were investigated using an AUTOLAB PGSTAT302N electrochemical workstation.

Conflict of Interest: The authors declare no competing financial interest.

Acknowledgment. This research was supported by the Basic Science Research Program through the National Research Foundation of Korea (NRF) funded by the Ministry of Science, ICT & Future Planning (2013R1A2A2A01068926).

Supporting Information Available: Additional discussions and figures of the structure and electrochemical properties of MnO_2 nanowires, self-charging and discharging performance

of SCSPCs at different applied forces, and self-charging performance of SCSPCs at reverse connection. This material is available free of charge *via* the Internet at http://pubs.acs.org.

REFERENCES AND NOTES

1. Yu, X.; Lu, B.; Xu, Z. Super Long-Life Supercapacitors Based on the Construction of Nanohoneycomb-like Strongly Coupled $CoMoO_4$-3D Graphene Hybrid Electrodes. *Adv. Mater.* **2014**, *26*, 1044–1051.
2. Wang, H.; Dai, H. Strongly Coupled Inorganic–Nano-Carbon Hybrid Materials for Energy Storage. *Chem. Soc. Rev.* **2013**, *42*, 3088–3113.
3. Rosa, E. A.; Dietz, T. Human Drivers of National Greenhouse-Gas Emissions. *Nat. Clim. Change* **2012**, *2*, 581–586.
4. Chu, S.; Majumdar, A. Opportunities and Challenges for a Sustainable Energy Future. *Nature* **2012**, *488*, 294–303.
5. Arico, A. S.; Bruce, P.; Scrosati, B.; Tarascon, J. M.; Van Schalkwijk, W. Nanostructured Materials for Advanced Energy Conversion and Storage Devices. *Nat. Mater.* **2005**, *4*, 366–377.
6. Tarascon, J. M.; Armand, M. Review Article Issues and Challenges Facing Rechargeable Lithium Batteries. *Nature* **2001**, *414*, 359–367.
7. Wang, Z. L. Towards Self-Powered Nanosystems: From Nanogenerators to Nanopiezotronics. *Adv. Funct. Mater.* **2008**, *18*, 3553–3567.
8. Hu, Y. F.; Zhang, Y.; Xu, C.; Lin, L.; Snyder, R. L.; Wang, Z. L. Self-Powered System with Wireless Data Transmission. *Nano Lett.* **2011**, *11*, 2572–2577.
9. Yang, R. S.; Qin, Y.; Dai, L. M.; Wang, Z. L. Power Generation with Laterally Packaged Piezoelectric Fine Wires. *Nat. Nanotechnol.* **2009**, *4*, 34–39.
10. Saravanakumar, B.; Mohan, R.; Thiyagarajan, K.; Kim, S. J. Fabrication of a ZnO Nanogenerator for Eco-Friendly Biomechanical Energy Harvesting. *RSC Adv.* **2013**, *3*, 16646–16656.
11. Wang, Z. L.; Song, J. H. Piezoelectric Nanogenerators Based on Zinc Oxide Nanowire Arrays. *Science* **2006**, *312*, 242–246.
12. Wang, Z. L. Self-Powered Nanotech. *Sci. Am.* **2008**, *298*, 82–87.
13. Wang, Z. L.; Wu, W. Nanotechnology-Enabled Energy Harvesting for Self-Powered Micro-/Nanosystems. *Angew. Chem., Int. Ed.* **2012**, *51*, 11700–11721.
14. Fan, F. R.; Tian, Z. Q.; Wang, Z. L. Flexible Triboelectric Generator. *Nano Energy* **2012**, *1*, 328–334.
15. Wang, Z. L. Triboelectric Nanogenerators as New Energy Technology for Self-Powered Systems and as Active Mechanical and Chemical Sensors. *ACS Nano* **2013**, *7*, 9533–9557.
16. Zhu, Y.; Murali, S.; Stoller, M. D.; Ganesh, K. G.; Cai, W.; Ferreira, P. J.; Pirkle, A.; Wallace, R. M.; Cychosz, K. A.; Thommes, M.; et al. Carbon-Based Supercapacitors Produced by Activation of Graphene. *Science* **2011**, *332*, 1537–1541.
17. Liu, C.; Yu, Z.; Neff, D.; Zhamu, A.; Jang, B. Z. Graphene-Based Supercapacitor with an Ultrahigh Energy Density. *Nano Lett.* **2010**, *10*, 4863–4868.
18. Chou, J. C.; Chen, Y. L.; Yang, M. H.; Chen, Y. Z.; Lai, C. C.; Chiu, H. T.; Lee, C. Y.; Chueh, Y. L.; Gan, J. Y. RuO_2/MnO_2 Core–Shell Nanorods for Supercapacitors. *J. Mater. Chem. A* **2013**, *1*, 8753–8758.
19. Lee, M.; Balasingam, S. K.; Jeong, H. Y.; Hong, W. G.; Kim, B. H.; Jun, Y. One-Step Hydrothermal Synthesis of Graphene Decorated V_2O_5 Nanobelts for Enhanced Electrochemical Energy Storage. *Sci. Rep.* **2015**, *5*, 8151–8158.
20. Xue, X.; Wang, S.; Guo, W.; Zhang, Y.; Wang, Z. L. Hybridizing Energy Conversion and Storage in a Mechanical-to-Electrochemical Process for Self-Charging Power Cell. *Nano Lett.* **2012**, *12*, 5048–5054.
21. Xue, X.; Deng, P.; Yuan, S.; Nie, Y.; He, B.; Xing, L.; Zhang, Y. CuO/PVDF Nanocomposite Anode for a Piezo-Driven Self-Charging Lithium Battery. *Energy Environ. Sci.* **2013**, *6*, 2615–2620.
22. Xue, X.; Deng, P.; He, B.; Nie, Y.; Xing, L.; Zhang, Y.; Wang, Z. L. Flexible Self-Charging Power Cell for One-Step Energy Conversion and Storage. *Adv. Energy Mater.* **2014**, *4*, 1301329.
23. Zhang, Y.; Zhang, Y.; Xue, X.; Cui, C.; He, B.; Nie, Y.; Deng, P.; Wang, Z. L. PVDF–PZT Nanocomposite Film Based Self-Charging Power Cell. *Nanotechnology* **2014**, *25*, 105401–105407.
24. Xing, L.; Nie, Y.; Xue, X.; Zhang, Y. PVDF Mesoporous Nanostructures as the Piezo-Separator for a Self-Charging Power Cell. *Nano Energy* **2014**, *10*, 44–52.
25. Kim, Y. S.; Xie, Y.; Wen, X.; Wang, S.; Kim, S. J.; Song, H. K.; Wang, Z. L. Highly Porous Piezoelectric PVDF Membrane as Effective Lithium Ion Transfer Channels for Enhanced Self-Charging Power Cell. *Nano Energy* **2015**, 10.1016/j.nanoen.2015.01.006.
26. Pankratov, D.; Falkman, P.; Blum, Z.; Shleev, S. A Hybrid Electric Power Device for Simultaneous Generation and Storage of Electric Energy. *Energy Environ. Sci.* **2014**, *7*, 989–993.
27. Pankratov, D.; Blum, Z.; Shleev, S. Hybrid Electric Power Biodevices. *ChemElectroChem* **2014**, *1*, 1798–1807.
28. Pankratov, D.; Blum, Z.; Suyatin, D. B.; Popov, V. O.; Shleev, S. Self-Charging Electrochemical Biocapacitor. *ChemElectroChem* **2014**, *1*, 343–346.
29. Yuan, C.; Hou, L.; Yang, L.; Li, D.; Shen, L.; Zhang, F.; Zhang, X. Facile Interfacial Synthesis of Flower-like Hierarchical a-MnO_2 Sub-microspherical Superstructures Constructed by Two-Dimension Mesoporous Nanosheets and Their Application in Electrochemical Capacitors. *J. Mater. Chem.* **2011**, *21*, 16035–16041.
30. Yu, P.; Zhang, X.; Wang, D. L.; Wang, L.; Ma, Y. W. Shape-Controlled Synthesis of 3D Hierarchical MnO_2 Nanostructures for Electrochemical Supercapacitors. *Cryst. Growth Des.* **2009**, *9*, 528–533.
31. Sung, D. Y.; Kim, I. Y.; Kim, T. W.; Song, M. S.; Hwang, S. J. Room Temperature Synthesis Routes to the 2D Nanoplates and 1D Nanowires/Nanorods of Manganese Oxides with Highly Stable Pseudocapacitance Behaviors. *J. Phys. Chem. C* **2011**, *115*, 13171–13179.
32. Ramadoss, A.; Kim, S. J. Hierarchically Structured TiO_2@MnO_2 Nanowall Arrays as Potential Electrode Material for High-Performance Supercapacitors. *Int. J. Hydrogen Energy* **2014**, *39*, 12201–12212.
33. Wei, W.; Cui, X.; Chen, W.; Ivey, D. J. Manganese Oxide-Based Materials as Electrochemical Supercapacitor Electrodes. *Chem. Soc. Rev.* **2011**, *40*, 1697–1721.
34. Bard, A. J.; Faulkner, L. R. *Electrochemical Methods: Fundamentals and Applications*, 2nd ed.; John Wiley & Sons, Inc.: New York, 2001.
35. Yu, H.; Huang, T.; Lu, M.; Mao, M.; Zhang, Q.; Wang, H. Enhanced Power Output of an Electrospun PVDF/MWCNTs-Based Nanogenerator by Tuning Its Conductivity. *Nanotechnology* **2013**, *24*, 405401–405409.
36. Lee, M.; Chen, C. Y.; Wang, S.; Cha, S. N.; Park, Y. J.; Kim, J. M.; Chou, L. J.; Wang, Z. L. A Hybrid Piezoelectric Structure for Wearable Nanogenerators. *Adv. Mater.* **2012**, *24*, 1759–1764.
37. Saravanakumar, B.; Soyoon, S.; Kim, S. J. Self-Powered pH Sensor Based on a Flexible Organic–Inorganic Hybrid Composite Nanogenerator. *ACS Appl. Mater. Interfaces* **2014**, *6*, 13716–13723.
38. Yuan, L.; Lu, X. H.; Xiao, X.; Zhai, T.; Dai, J.; Zhang, F.; Hu, B.; Wang, X.; Gong, L.; Chen, J.; et al. Flexible Solid-State Supercapacitors Based on Carbon Nanoparticles/MnO_2 Nanorods Hybrid Structure. *ACS Nano* **2012**, *6*, 656–661.
39. Meng, C.; Liu, C.; Chen, L.; Hu, C.; Fan, S. Highly Flexible and All-Solid-State Paper-like Polymer Supercapacitors. *Nano Lett.* **2010**, *10*, 4025–4031.
40. Xiong, G.; Meng, C.; Reifenberger, R. G.; Irazoqui, P. P.; Fisher, T. S. Graphitic Petal Electrodes for All-Solid-State Flexible Supercapacitors. *Adv. Energy Mater.* **2014**, *4*, 1300515–1300524.
41. Yang, P.; Xiao, X.; Li, Y.; Ding, Y.; Qiang, P.; Tan, X.; Mai, W.; Lin, Z.; Wu, W.; Li, T.; et al. Hydrogenated ZnO Core–Shell Nanocables for Flexible Supercapacitors and Self-Powered Systems. *ACS Nano* **2013**, *7*, 2617–2626.